Electronic Supporting Information

Synthesis of steroidal molecular compasses: Exploration on the controlled assembly of solid organic materials

Nancy Aguilar-Valdez,[a] Mauricio Maldonado-Domínguez,[a] Rafael Arcos-Ramos,[b*]
Margarita Romero-Ávila,[a] Rosa Santillan,[c] and Norberto Farfán [a*]

[a] *Facultad de Química, Departamento de Química Orgánica, Universidad Nacional Autónoma de México, 04510 Ciudad de México, México. E-mail: norberto.farfan@gmail.com*

[b] *Departamento de Química y Radioquímica, Instituto de Ciencias Nucleares, Universidad Nacional Autónoma de México, 04510 Ciudad de México, México. E-mail: rafaelarcos84@gmail.com*

[c] *Departamento de Química, Centro de Investigación y de Estudios Avanzados del IPN, Ciudad de México. Apdo. Postal 14-740, 07000, México.*

Contents **Page**

Crystal data and structure refinement for compounds **8** and **11** **2**
Synthesis of 2,5-dibromo-4-aniline **4**
Selected chemical shifts for *p*-nitroaniline ring in steroidal derivatives **7-11** **4**
^{1}H-NMR and ^{13}C-NMR spectra of compound **7** **6**
^{1}H-NMR and ^{13}C-NMR spectra of compound **8** **8**
^{1}H-NMR and ^{13}C-NMR spectra of compound **9** **10**
^{1}H-NMR and ^{13}C-NMR spectra of compound **10** **12**
^{1}H-NMR and ^{13}C-NMR spectra of compound **11** **14**
Theoretical band structure and density of states for self-assembled solid derived from compound **8** **16**
Modeling recognition of small molecules in a crystal from steroidal compass **11** **17**

Table S1. Crystal data and structure refinement for compounds **8** and **11.**

Compound	**8**	**11**
Physical appearance	Yellow needles	Yellow needles
Empirical formula	$C_{48}\ H_{54}\ N_2\ O_6$	$C_{48}\ H_{62}\ N_2\ O_4$
Formula weight	754.93	731.00
Space group	$P\ 2_1 2_1 2_1$	C 2
Crystal system	Orthorhombic	Monoclinic
a (Å)	11.8249 (2)	39.1690 (8)
b (Å)	13.9462 (3)	7.5511 (15)
c (Å)	26.1937 (5)	16.7020 (3)
α (°)	90.0	90.0
β (°)	90.0	95.27 (3)
γ (°)	90.0	90.0
Volume ($Å^3$)	4319.37 (14)	4918.9 (17)
Z	4	8
Crystal size (mm^3)	0.28 x 0.20 x 0.15	0.38 x 0.25 x 0.18
Temperature (K)	173 (2)	293 (2)
δ (mg/m^3)	1.161	0.987
Absorption coefficient (mm^{-1})	0.076	0.062
F (000)	1616	1584
θ range for data collection (°)	2.921 to 27.457	4.615 to 27.641
Index ranges	$-15 \le h \le 12$ $-18 \le k \le 18$ $-35 \le l \le 33$	$-50 \le h \le 44$ $-9 \le k \le 9$ $-20 \le l \le 21$
Reflections collected	9642	10522
Refinement method	Full-matrix least-squares on F^2	
Goodness-of-fit on F^2	1.030	1.012
Data/Restraints/Parameters	9642/2/574	10522/77/497
Final R índices [I>2sigma(I)]	$R_1 = 0.0547$ $wR_2 = 0.1386$	$R_1 = 0.0873$ $wR_2 = 0.2242$
R indices (*all data*)	$R_1 = 0.0843$ $wR_2 = 0.1544$	$R_1 = 0.1544$ $wR_2 = 0.2703$

Table S2. Hydrogen bonds for derivative **11** [Å and °].

D-H...A	d(D-H)	d(H...A)	d(D...A)	<(DHA)
O(1)-H(1A)...O(2)#1	0.82	2.07	2.868(5)	166.1
O(2)-H(2B)...N(2)#2	0.871(14)	2.623(18)	3.490(9)	174(5)
O(2)-H(2B)...O(3)#2	0.871(14)	2.37(3)	3.134(10)	147(5)
O(2)-H(2B)...O(4)#2	0.871(14)	2.21(3)	3.032(10)	158(5)
O(1)-H(1A)...O(2)#1	0.82	2.07	2.868(5)	166.1
O(2)-H(2B)...N(2)#2	0.871(14)	2.623(18)	3.490(9)	174(5)
O(2)-H(2B)...O(3)#2	0.871(14)	2.37(3)	3.134(10)	147(5)
O(2)-H(2B)...O(4)#2	0.871(14)	2.21(3)	3.032(10)	158(5)

Symmetry transformations used to generate equivalent atoms: #1 -x+1,y+1,-z+1 #2 x,y-1,z

1. Synthesis of 2,5-dibromo-4-nitroaniline (**1**)

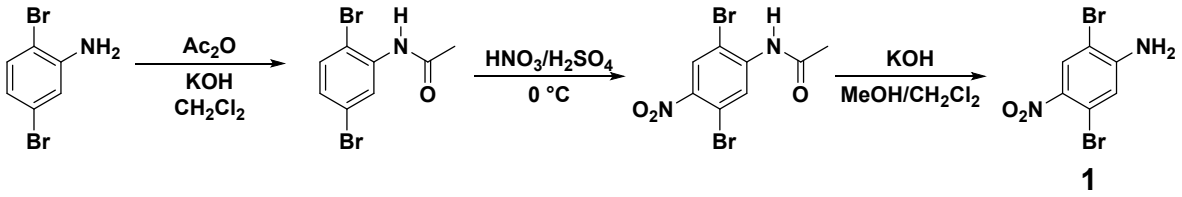

Synthesis of N-(2,5-dibromophenyl)acetamide: To a solution of 2,5-dibromoaniline (10.0 mmol, 2.51 g), acetic anhydride (30.0 mmol, 2.8 mL) in CH_2Cl_2 (10 mL) was added an aqueous solution of KOH (2.0 g in 2 mL water). The reaction mixture was refluxed to 5 h. Then, the reaction was cooled down to room temperature; the obtained solid was isolated by vacuum filtration and washed with cold CH_2Cl_2 and H_2O. The crude product was purified by recrystallization using EtOH:H_2O (1:1) to afford *N*-(2,5-dibromophenyl)acetamide as white crystalline solid (1.24 g, 42 %). ^{1}H-NMR [300 MHz, Acetone-d6] (δ, ppm): 8.58 (br, 1H), 8.39 (d, *J* = 2.5 Hz, 1H), 7.56 (d, *J* 8.5 Hz, 1H), 7.23 (dd, *J* = 8.5 Hz, 1H), 2.21 (s, 3H).

Synthesis of N-(2,5-dibromo-4-nitrophenyl)acetamide: To a solution of *N*-(2,5-dibromophenyl)acetamide (17.0 mmol, 5.0 g) in H_2SO_4 (10 mL) was cooled to 0 °C on a ice-water bath. After, a solution of HNO_3/H_2SO_4 (6:4, 20 mL) was added dropwise during 1 h at low temperature. Then, the reaction mixture was poured into water:ice and the solid was isolated by vacuum filtration. The solid was dissolved in CH_2Cl_2 (100 mL) and washed with water (2 x 25 mL), 10 % KOH (2 x 25 mL) and brine (2 x 25 mL). The organic portion was dried over anhydrous Na_2SO_4 and the solvent was removed to dryness under vacuum. The crude product was purified by recrystallization in EtOH:Acetone (1:1) to afford *N*-(2,5-dibromo-4-nitrophenyl)acetamide as yellow crystalline solid (5.1 g, 89 %). ^{1}H-NMR [300 MHz, $CDCl_3$] (δ, ppm): 8.95 (s, 1H), 8.17 (s, 1H), 7.78 (s, 1H), 2.31 (s, 3H).

Synthesis of 2,5-dibromo-4-nitroaniline (1): To a solution of *N*-(2,5-dibromo-4-nitrophenyl)acetamide (6.0 mmol, 2.0 g) in THF/MeOH (1:1, 100 mL) was added KOH (0.5

g) and was stirred until consumption of starting materials. Then, H_2O (100 mL) was added; the obtained solid was isolated by vacuum filtration and washed with cold water. The crude product was purified by recrystallization in EtOH:Acetone (1:1) to afford 2,5-dibromo-4-nitroaniline as yellow crystalline solid (1.46 g, 82 %). ^{1}H-NMR [300 MHz, $CDCl_3$] (δ, ppm): 8.91 (s, 1H), 7.13 (s, 1H), 6.37 (br, 2H).

Compound	^{1}H NMR				^{13}C NMR						
	H-24	H-25	H-27	H-28	C-22	C-23	C-24	C-25	C-26	C-27	C-28
7[a]	8.05	****	6.95	****	138.4	153.8	130.4	121.3	107.3	118.6	****
8[b]	****	8.28	****	6.86	****	139.3	148.6	130.4	119.8	106.7	118.5
9[b]	8.09	****	6.74	****	138.7	151.9	130.2	120.5	106.9	118.1	****
10[b]	8.11	****	6.57	****	139.0	151.6	130.3	120.5	106.9	118.1	****
11[b]	8.15	****	6.79	****	139.3	151.2	130.1	120.5	107.0	118.0	****

Table S3. ^{1}H and ^{13}C NMR selected chemical shifts (δ, ppm) for *p*-nitroaniline ring in steroidal derivatives **7-11**. [a]Acetone-d_6 and [b]$CDCl_3$ (10 mg dissolved in 2 mL).

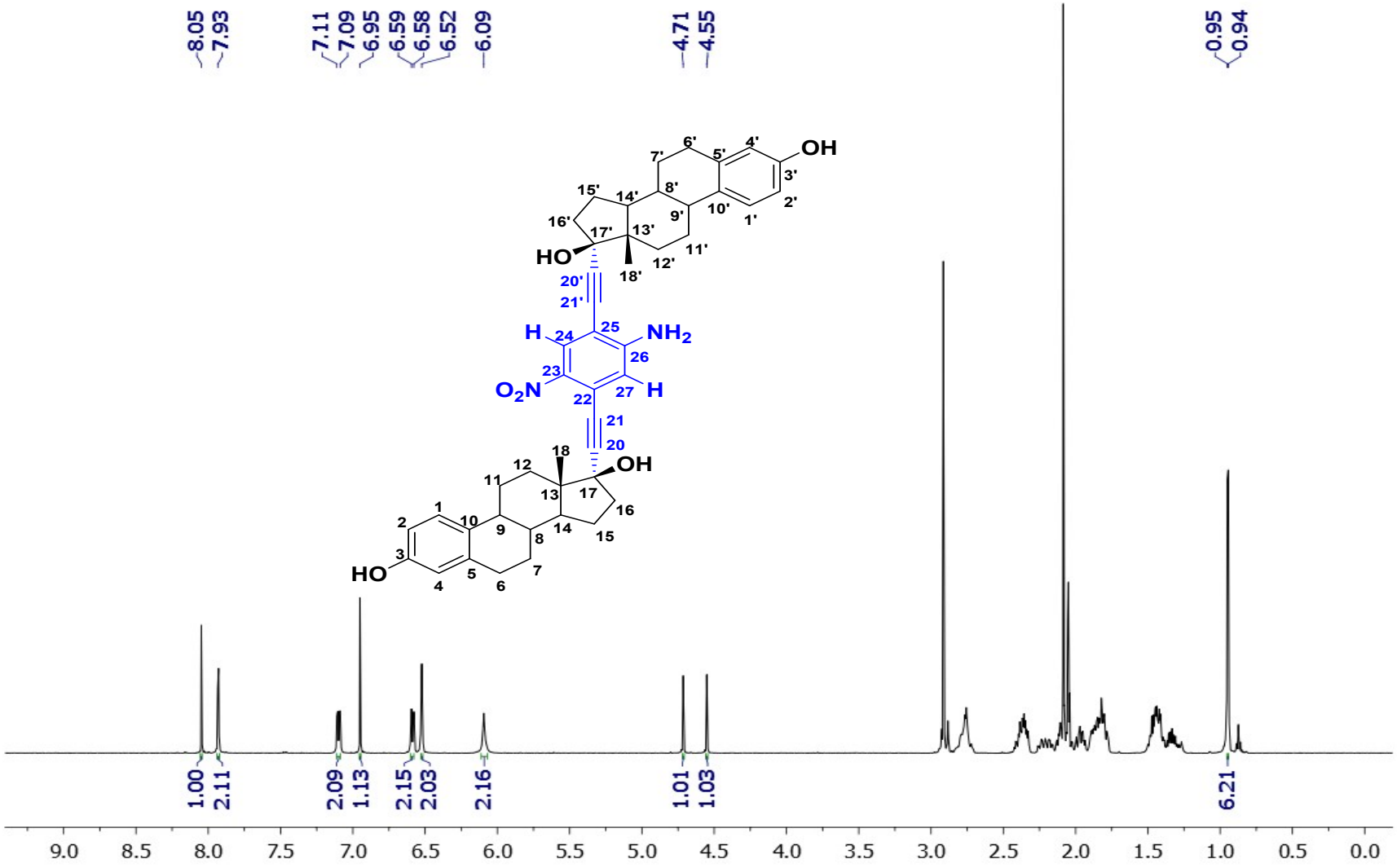

^{1}H-NMR spectrum of 2,5-Bis(17α-ethynyl-estra-1,3,5-(10)-trien-3-17β-diol)-4-nitroaniline (**7**)

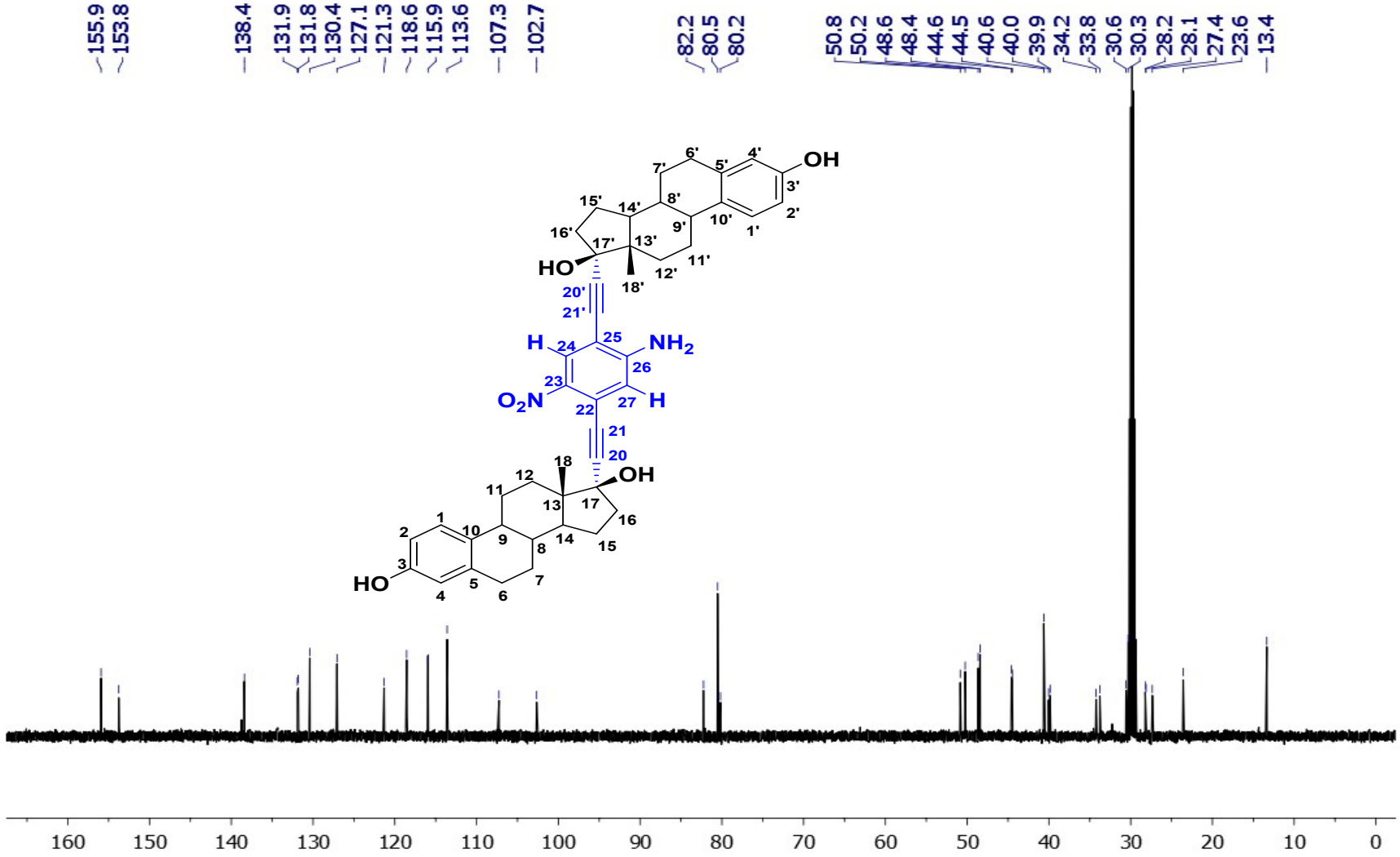

^{13}C-NMR spectrum of 2,5-Bis(17α-ethynyl-estra-1,3,5-(10)-trien-3-17β-diol)-4-nitroaniline (**7**)

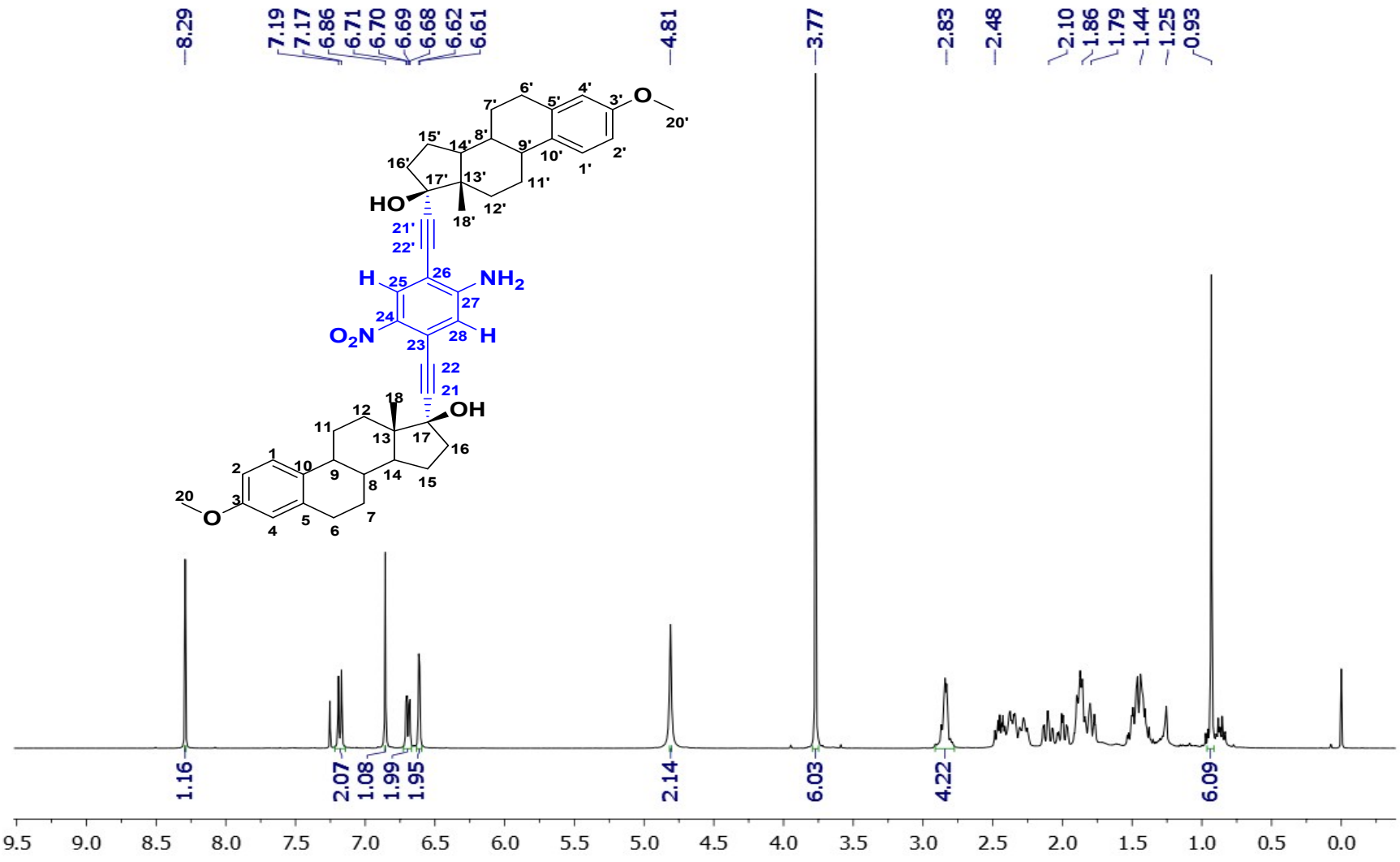

^{1}H-NMR spectrum of 2,5-Bis(17α-ethynyl-estra-1,3,5-(10)-trien-17β-ol-3-methyl ether)-4-nitroaniline (**8**)

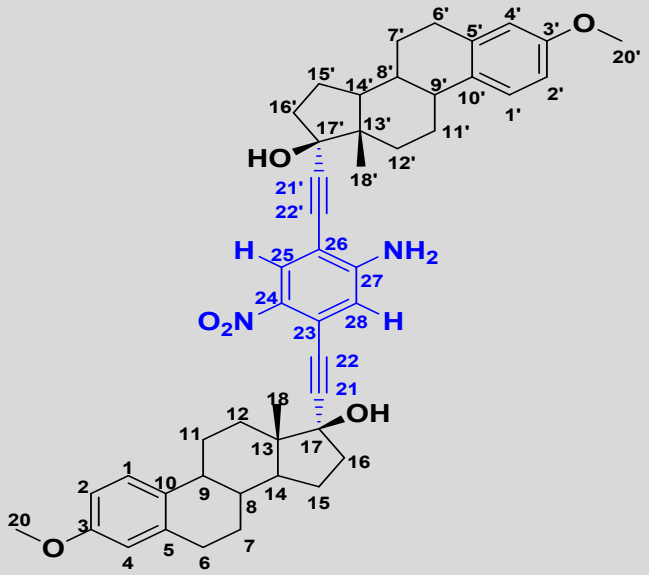

^{13}C-NMR spectrum of 2,5-Bis(17α-ethynyl-estra-1,3,5-(10)-trien-17β-ol-3-methyl ether)-4-nitroaniline (**8**)

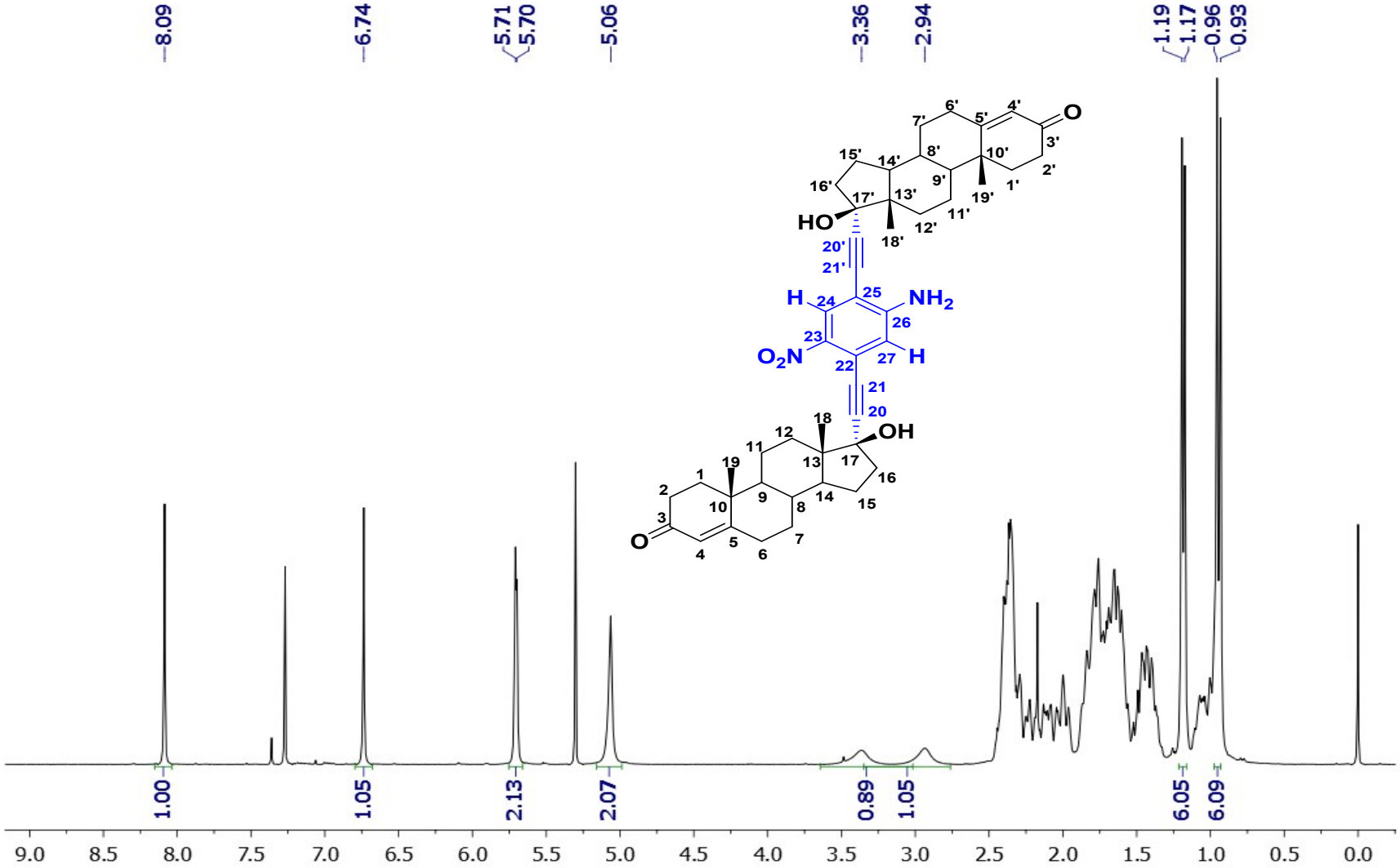

[1]H-NMR spectrum of 2,5-Bis(17α-ethynyl-17β-hydroxy-testosterone)-4-nitroaniline (**9**)

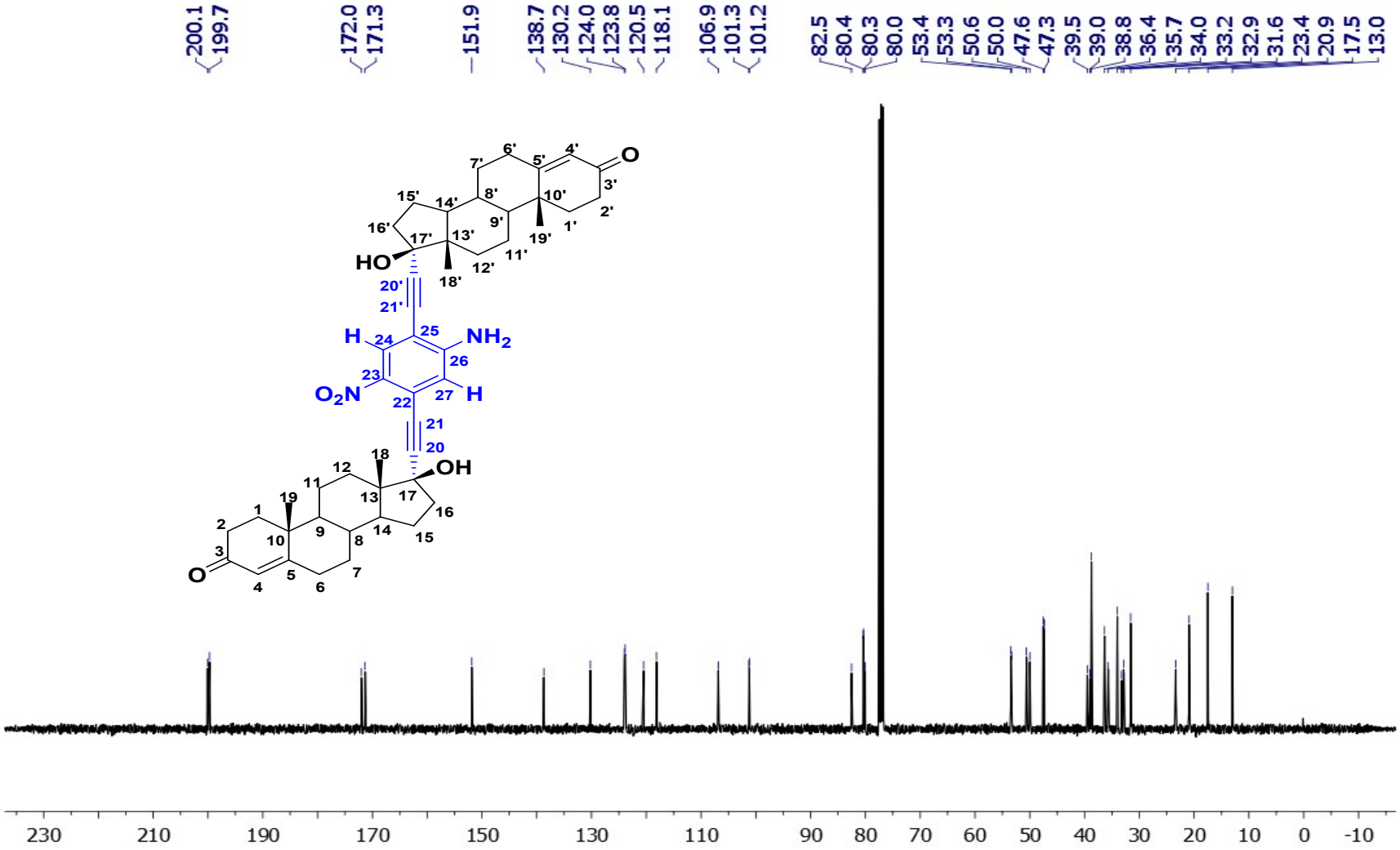

^{13}C-NMR spectrum of 2,5-Bis(17α-ethynyl-17β-hydroxy-testosterone)-4-nitroaniline (**9**)

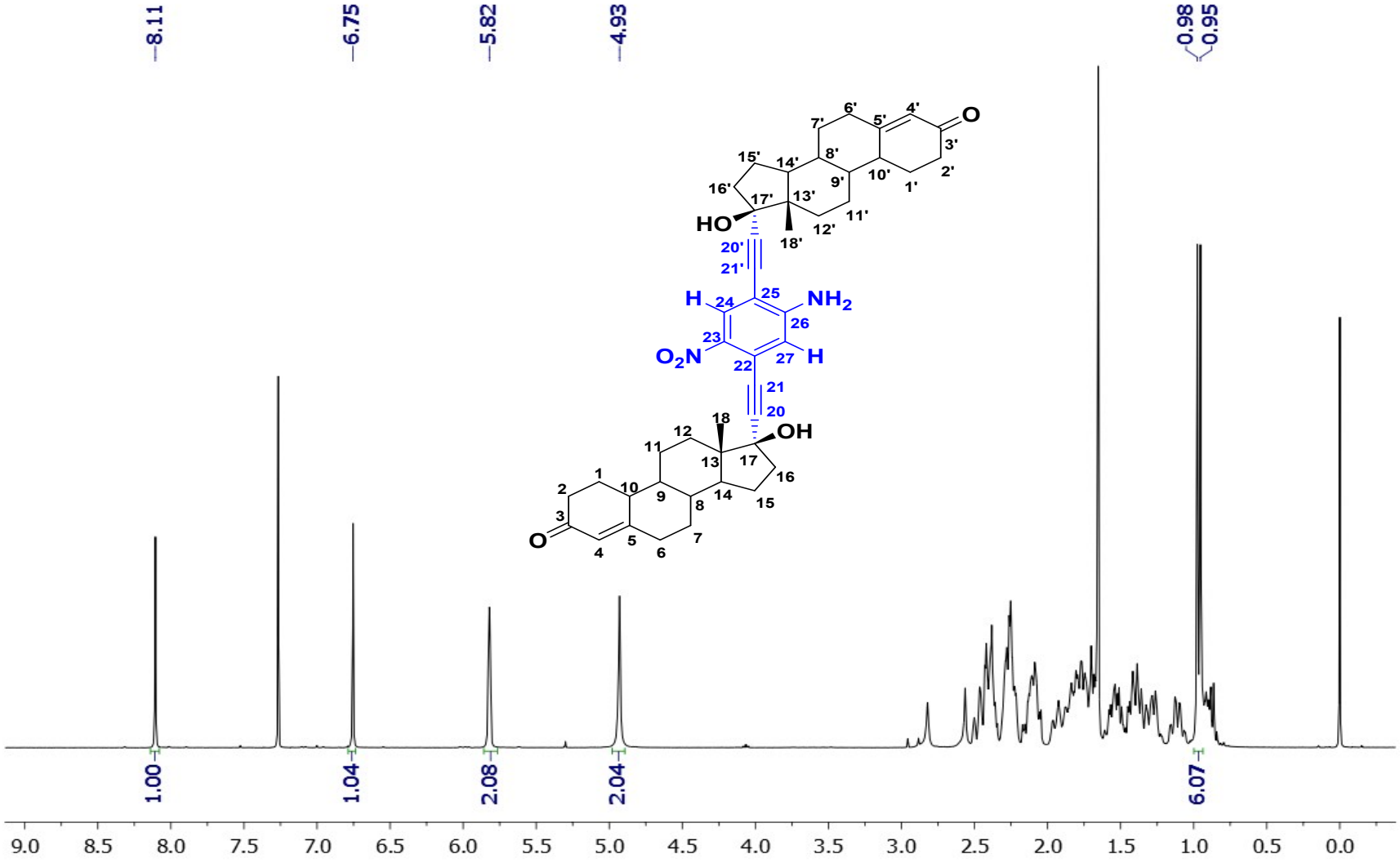

^{1}H-NMR spectrum of 2,5-Bis(19-nor-17α-ethynyl-17β-hydroxy-testosterone)-4-nitroaniline (**10**)

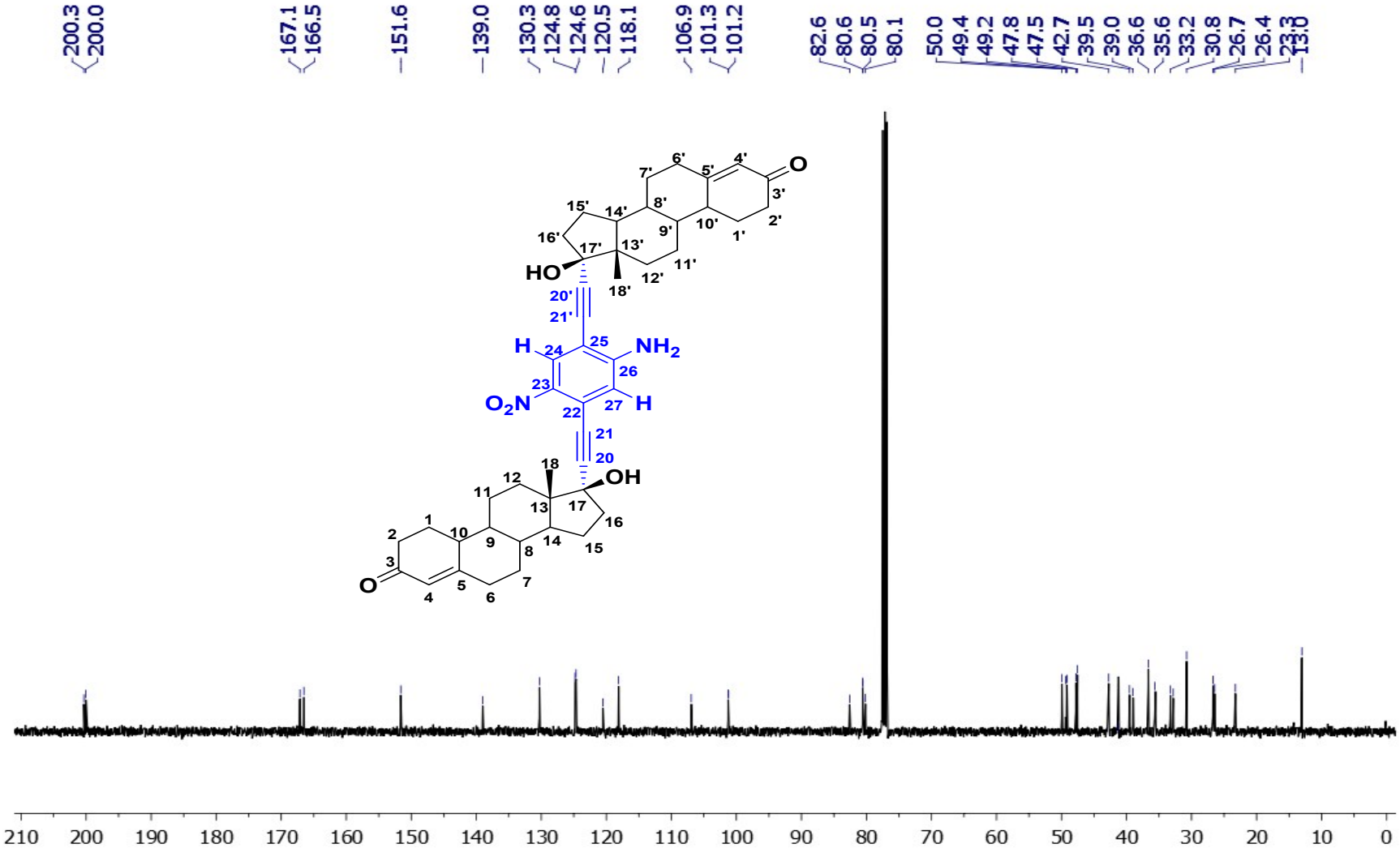

^{13}C-NMR spectrum of 2,5-Bis(19-nor-17α-ethynyl-17β-hydroxy-testosterone)-4-nitroaniline (**10**)

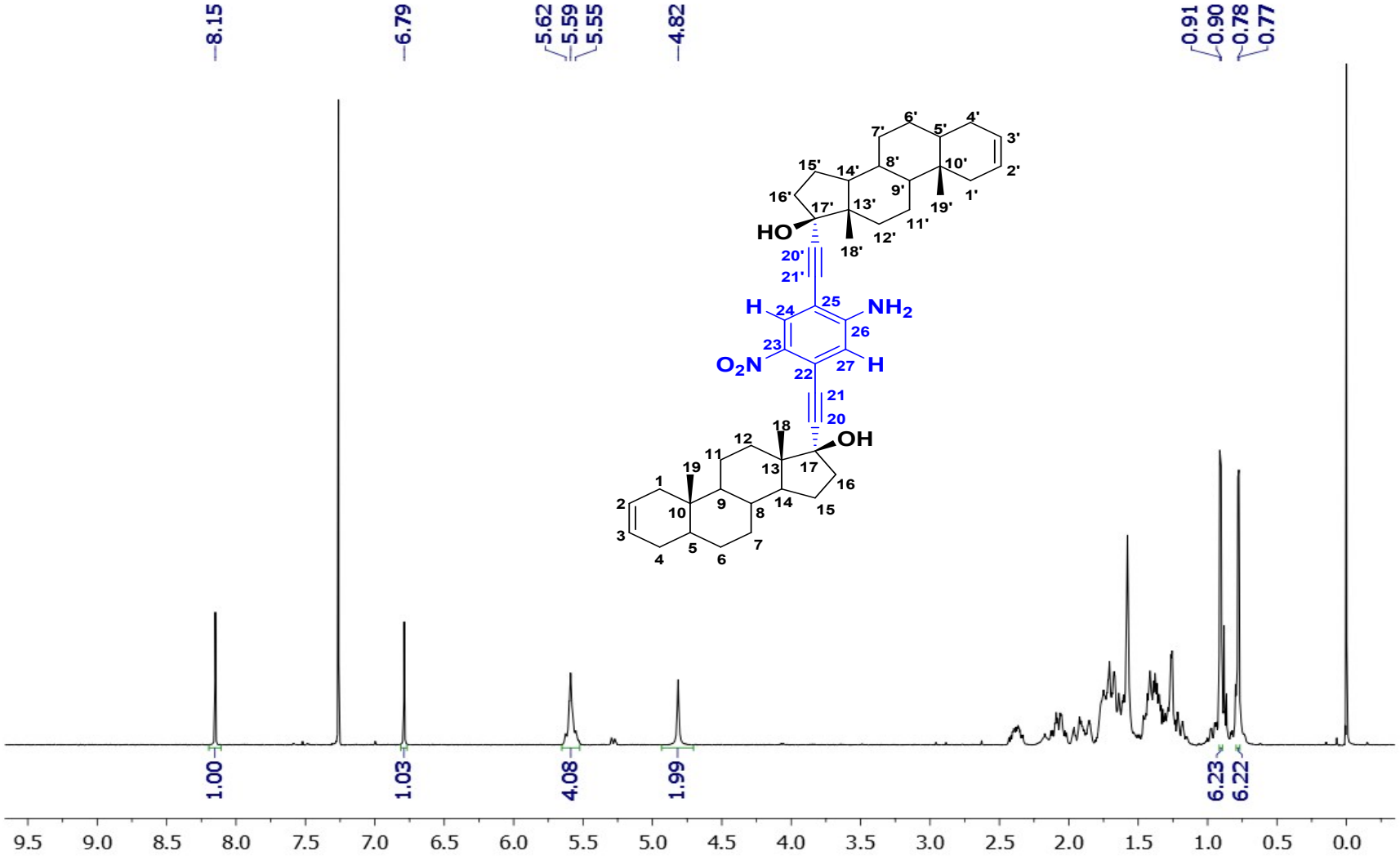

[1]H-NMR spectrum of 2,5-Bis(17α-ethynyl-5α-androst-2-en-17β-ol)-4-nitroaniline (**11**)

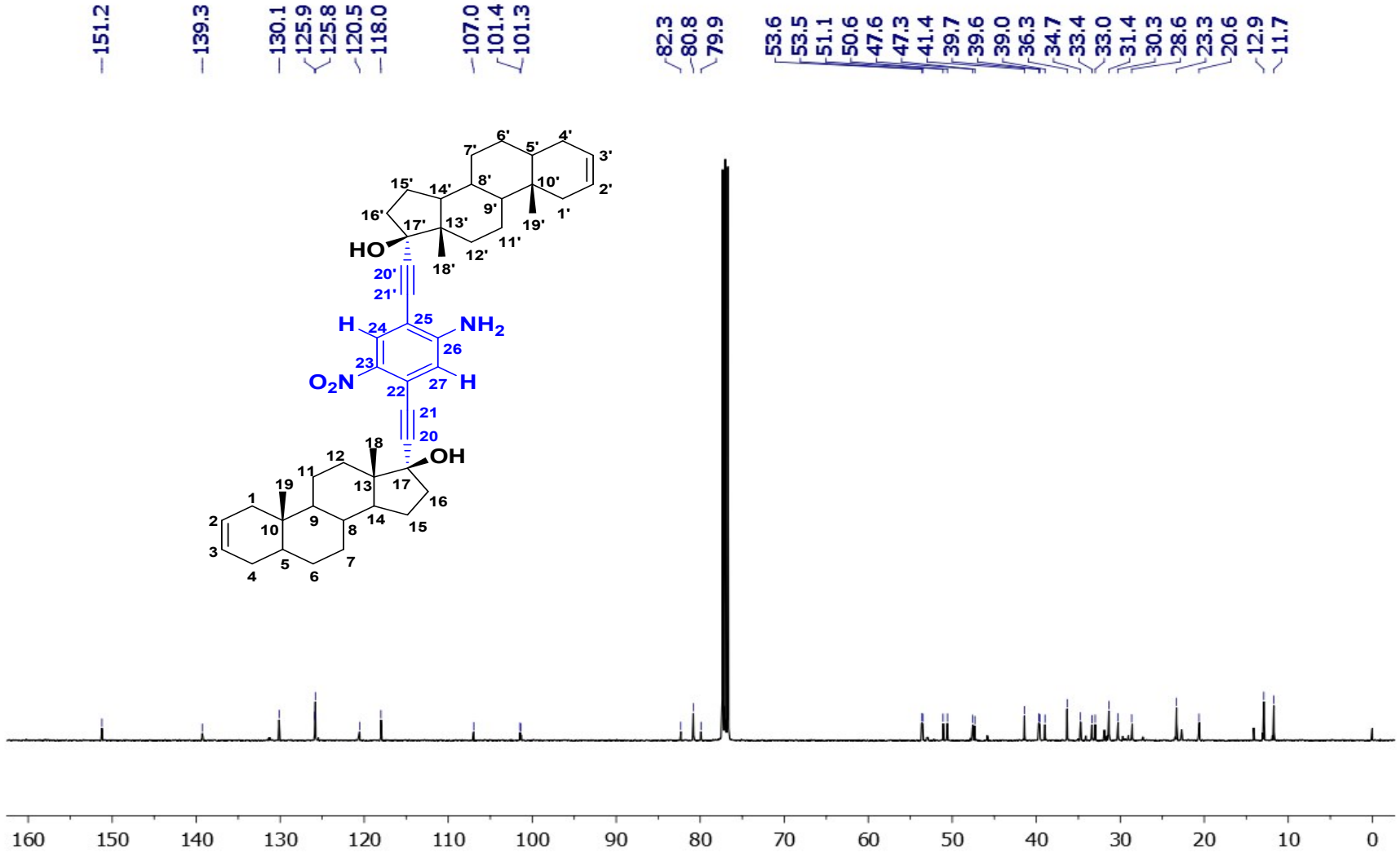

^{13}C-NMR spectrum of 2,5-Bis(17α-ethynyl-5α-androst-2-en-17β-ol)-4-nitroaniline (**11**)

Theoretical band structure and density of states for self-assembled solid derived from compound 8

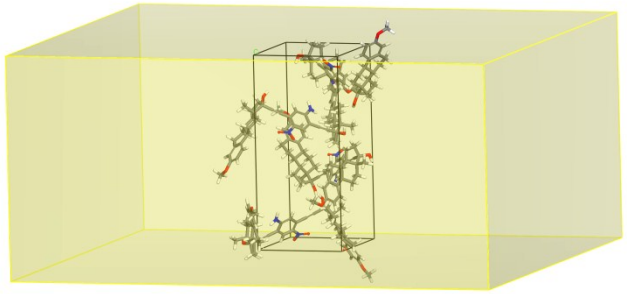

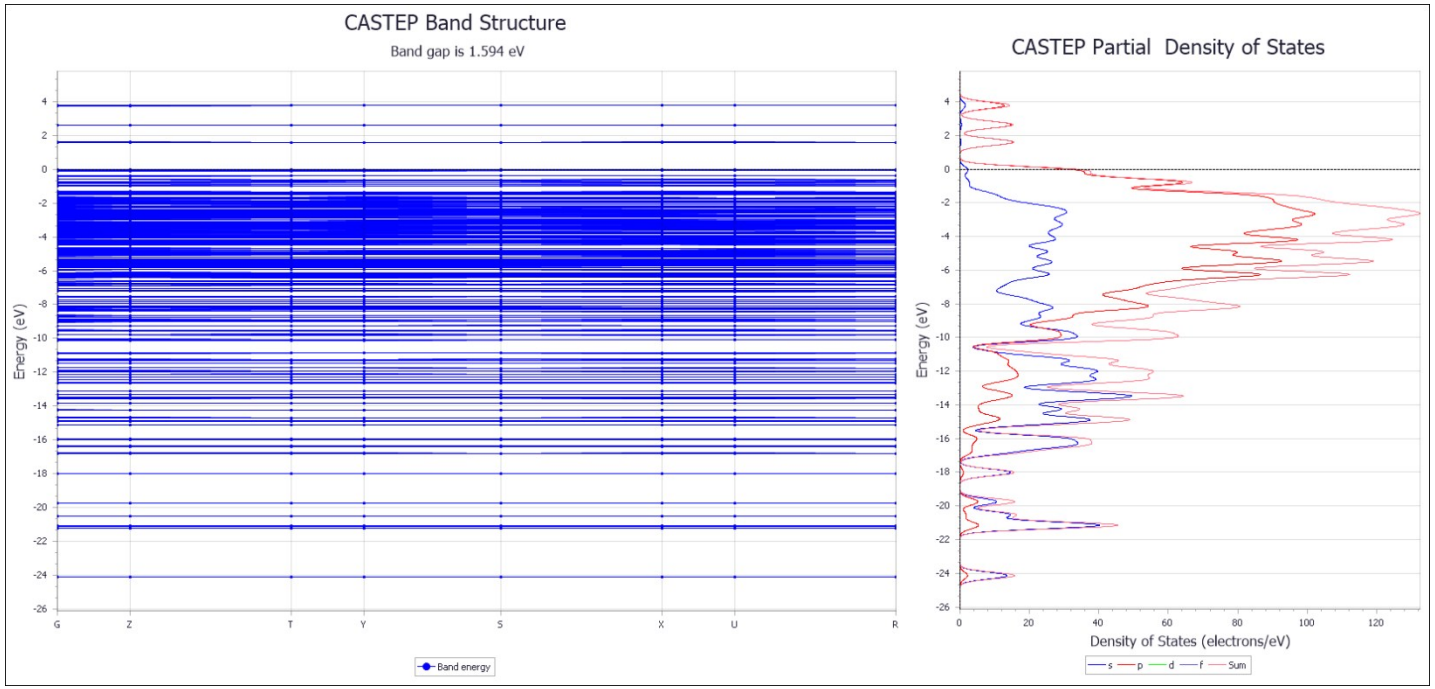

Modeling the recognition of small molecules in a crystal from derivative 11

The Sorption program, as Bundled within MS8, was used to simulate the absorption of small organic molecules (methane, ethane, ethylene, acetylene, carbon monoxide, carbon dioxide, carbonyl sulfide and benzene) in the porous network.

The COMPASS force field was used in this task, with its own set of atomic charges, using the Ewald & Group summation method and the Metropolis algorithm for Monte Carlo simulation of the absorption process. 10 fugacity steps were covered during this search, for each small molecule from 0.01 to 10 kPa; 1,000,000 equilibration steps and 10,000,000 production steps were employed for each fugacity step, ensuring a thorough sampling of the available sorption modes. Fugacity was sampled in logarithmically spaced steps, so a finer detail is captured at early stages of the sorption processes.

Recognition of small hydrocarbons: A low affinity of the porous solid for methane (CH_4) adsorption is predicted, and captured in the low density of molecules upon simulation, and in the corresponding adsoprtion isotherm, where no saturation can be devised within the fugacity interval sampled. Ethane (C_2H_6) shows increased adsorption in the pores of the self-assembled steroidal framework, and this becomes more pronounced when insaturations are introduced. Hence, simulation predicts a stronger binding for ethylene (C_2H_4) and acetylene (C_2H_2). Benzene (C_6H_6) is an exceptional system as observed from the Monte Carlo study, where high binding affinity (around -20 kcal/mol) is predicted. Its hydrophobic nature facilitates entering the cavities, whose size and shape are large enough to allocate this aromatic ring. Furthermore, planar stacking between the benzene rings and the 4-nitroaniline moieties contributes to further stabilize the loaded state. This solid is thus predicted to selectively recognize aromatic rings from a mixture of hidrocarbons.

Methane adsorption (CH_4):

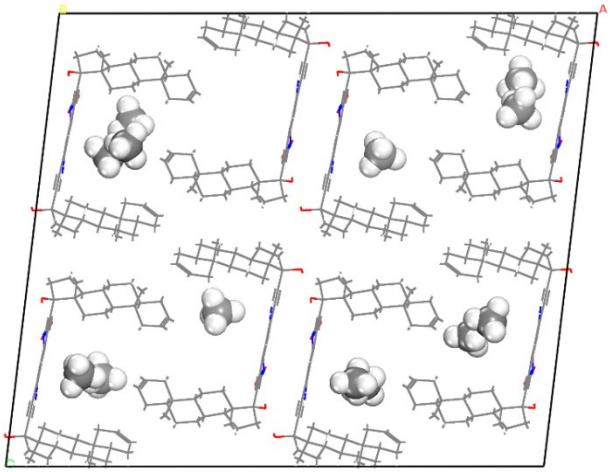

Front view of the channels present in the crystal from 11, loaded with CH_4

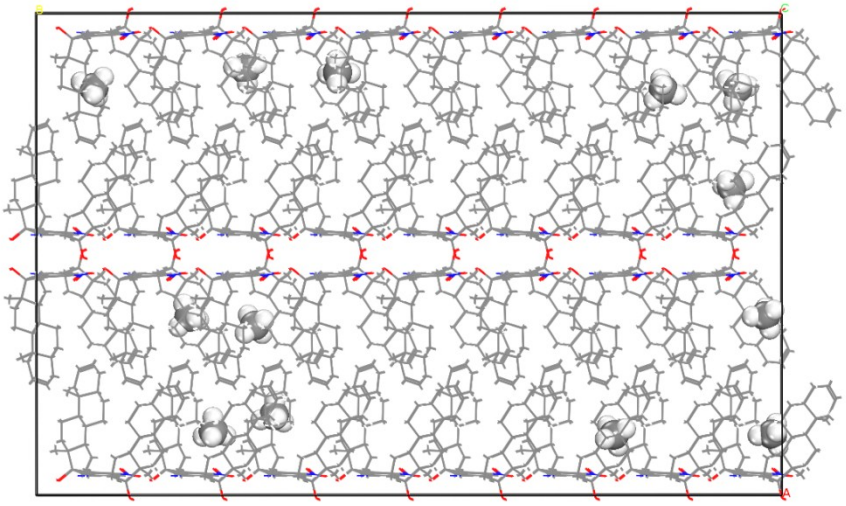

Top view of the channels present in the crystal from 11, loaded with CH_4

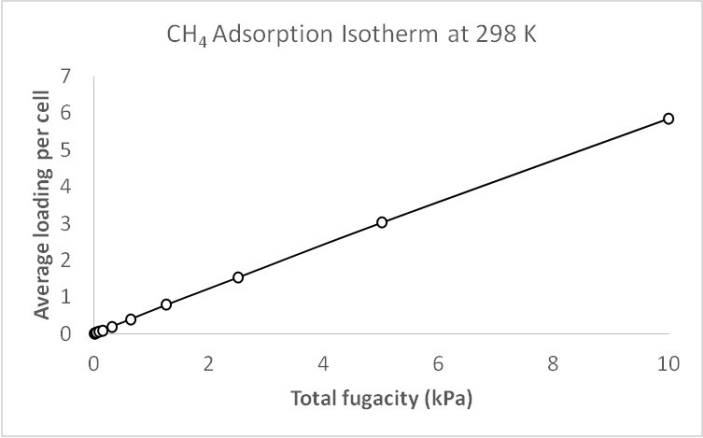

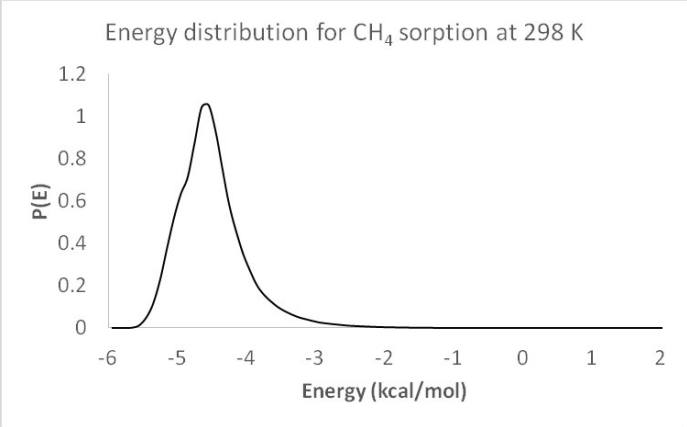

Ethane (C_2H_6) adsorption:

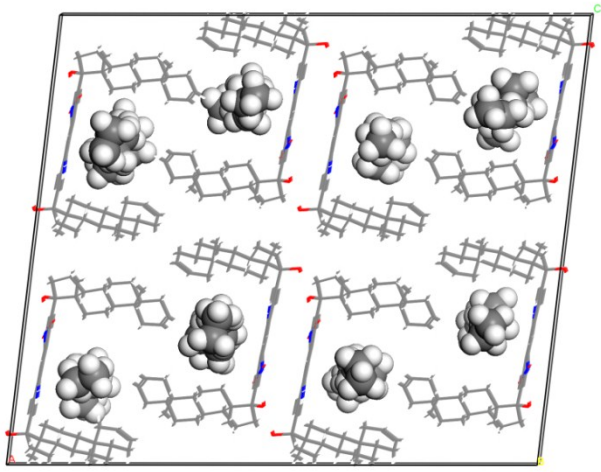

Front view of the channels present in the crystal from 11, loaded with C_2H_6

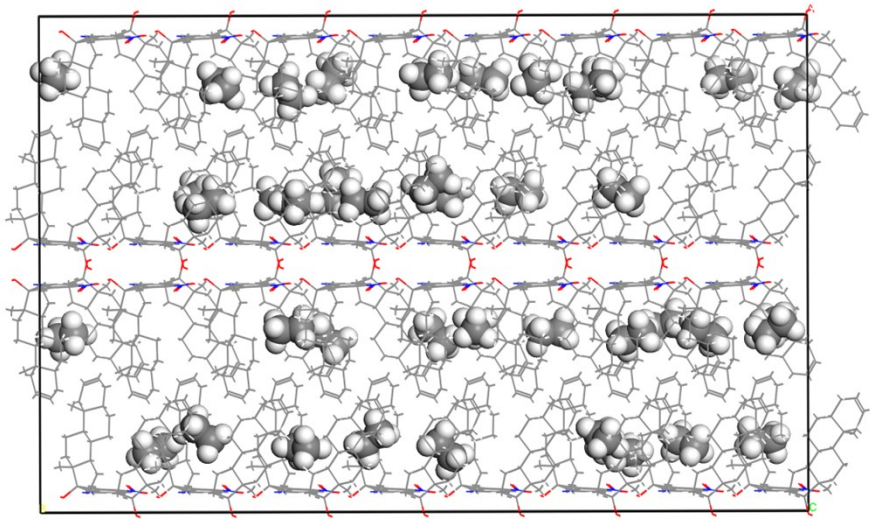

Top view of the channels present in the crystal from 11, loaded with C_2H_6

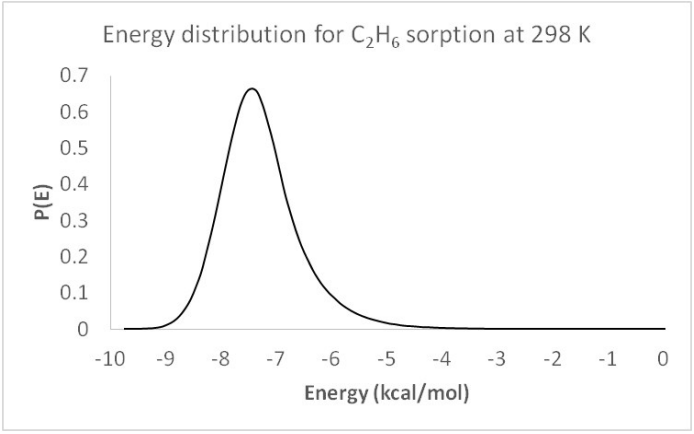

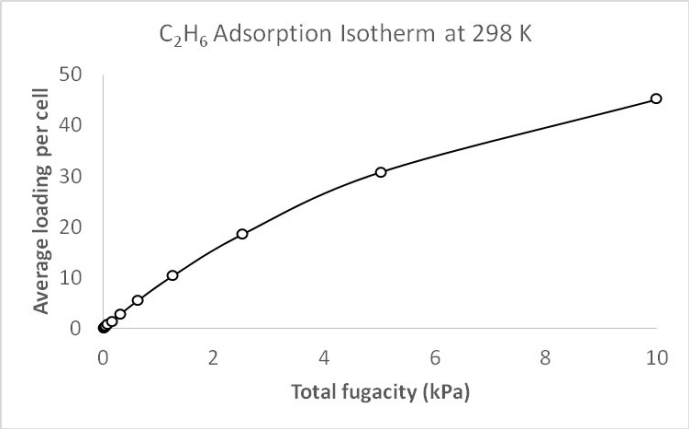

Ethylene (C_2H_4) adsorption:

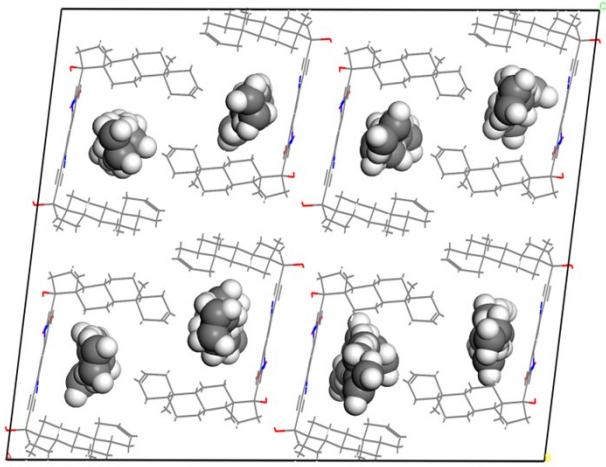

Front view of the channels present in the crystal from 11, loaded with C_2H_4

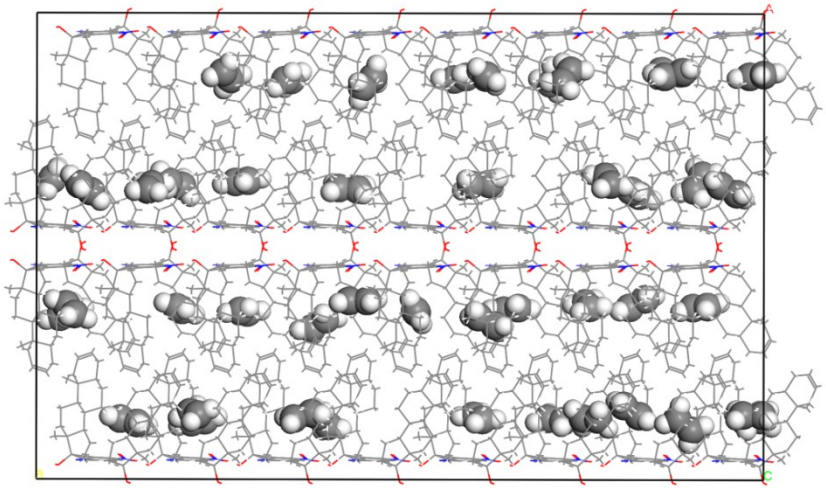

Top view of the channels present in the crystal from 11, loaded with C_2H_4

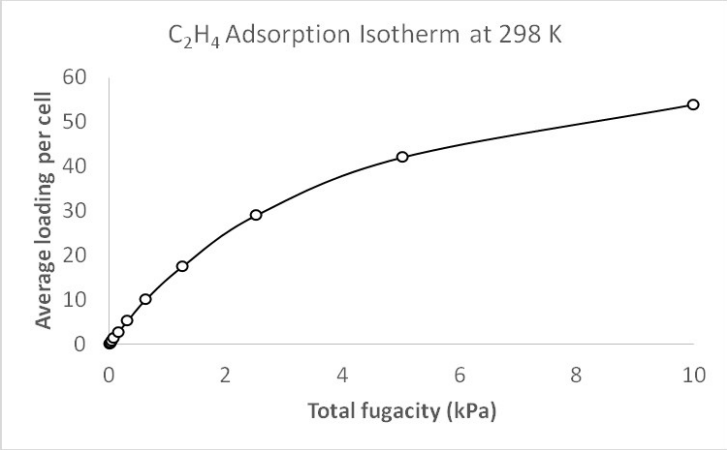

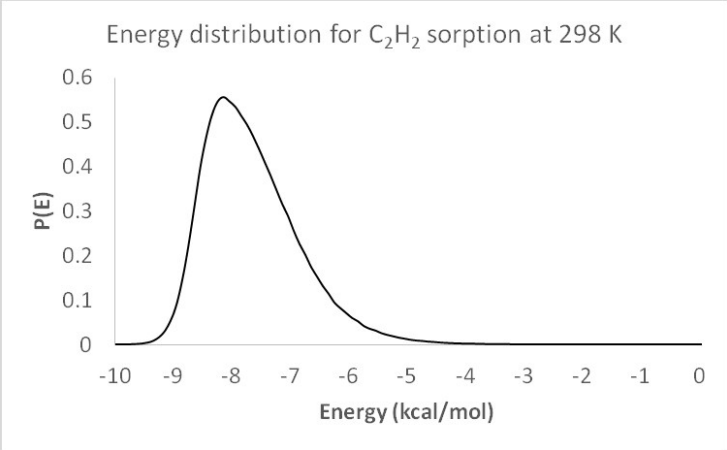

Acetylene (C_2H_2) adsorption:

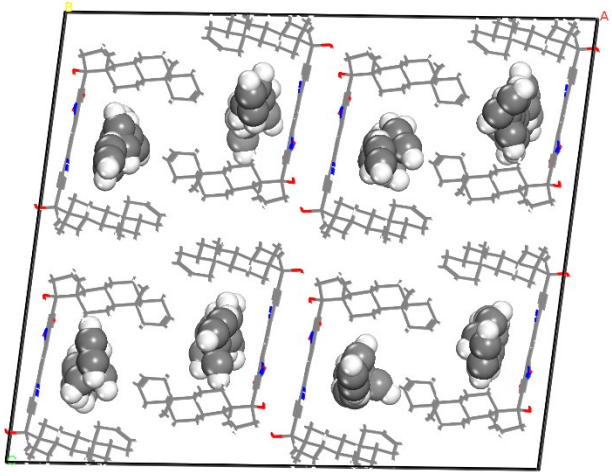

Front view of the channels present in the crystal from 11, loaded with C_2H_2

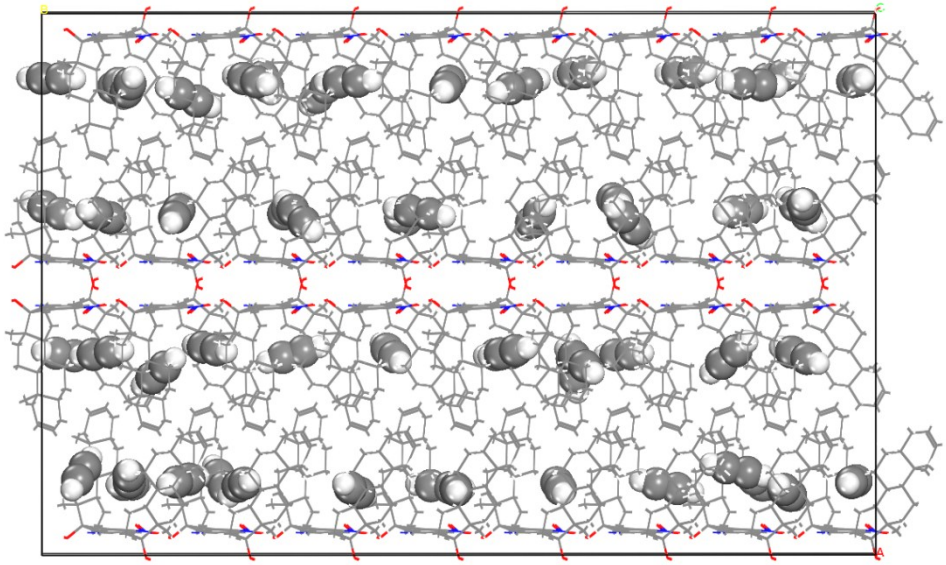

Top view of the channels present in the crystal from 11, loaded with C_2H_2

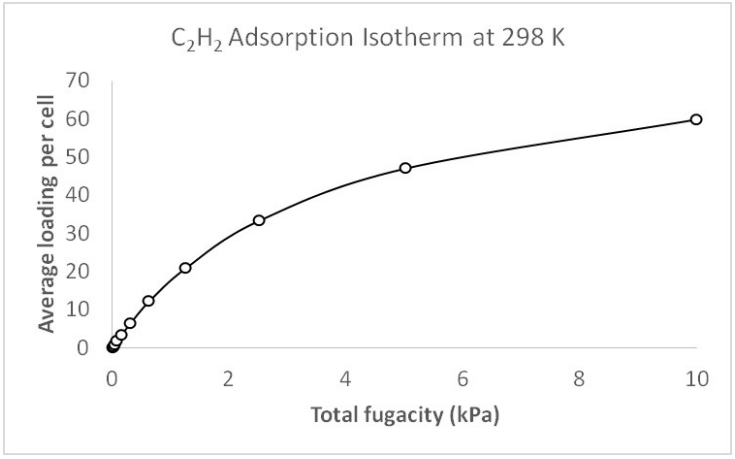

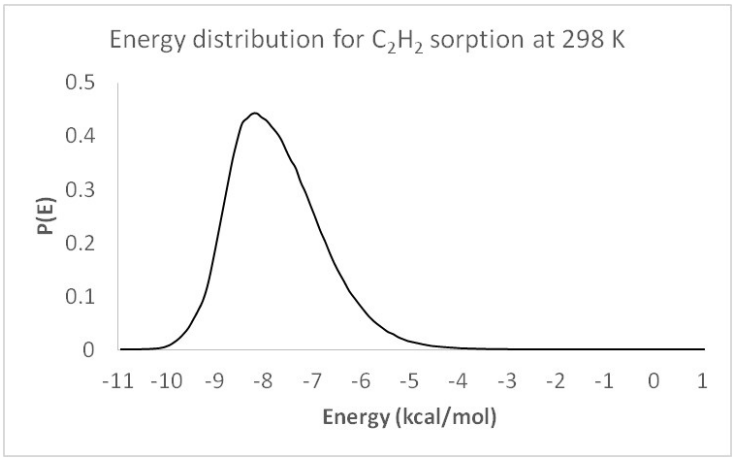

Benzene (C_6H_6) adsorption:

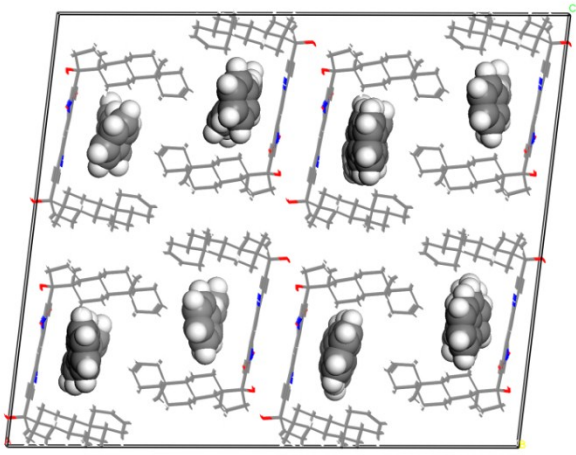

Front view of the channels present in the crystal from 11, loaded with C_6H_6

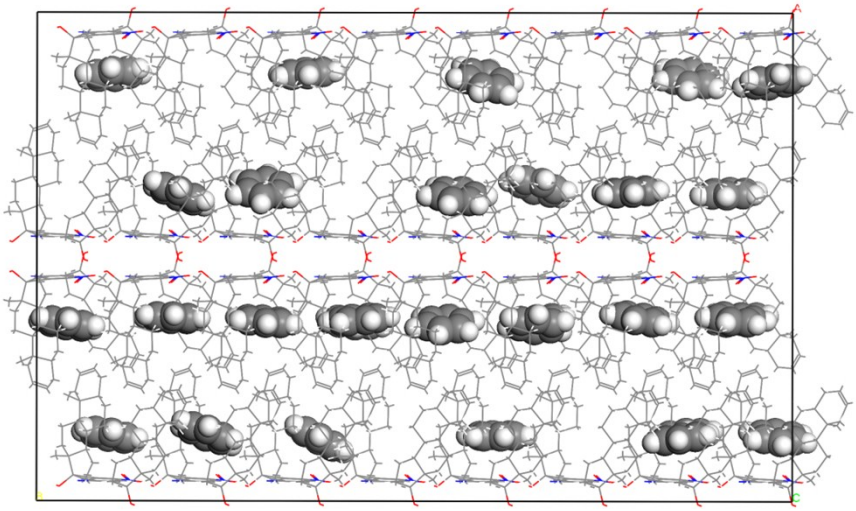

Top view of the channels present in the crystal from 11, loaded with C_6H_6

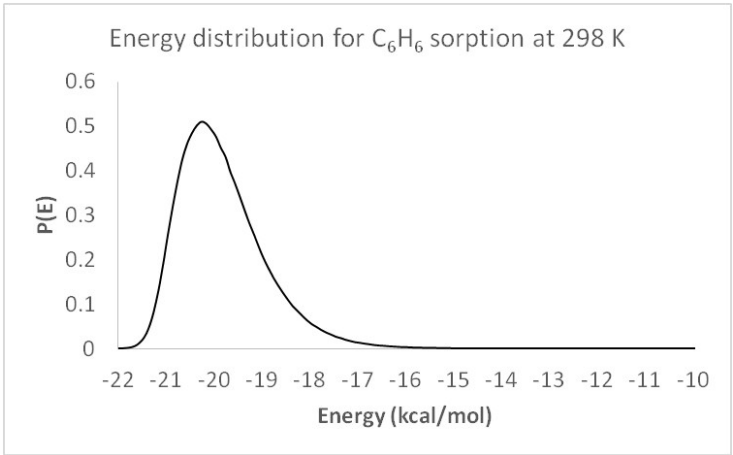

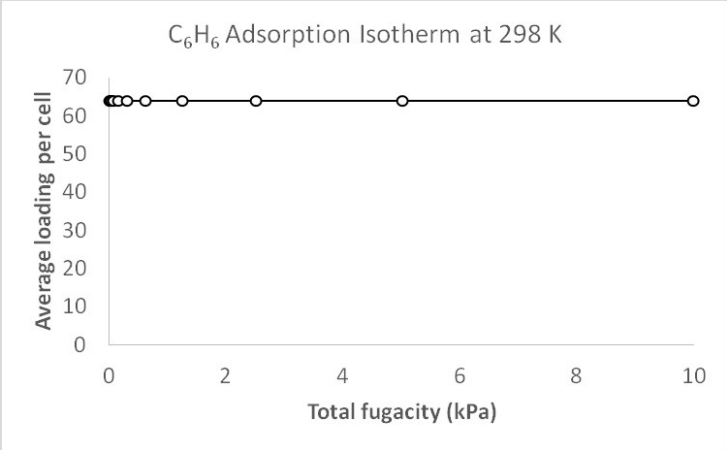

Adsorption of carbon chalcogenides: Carbon monoxide and carbon dioxide are molecules whose recognition and trapping are areas of growing interest. The toxicity of CO makes it necessary to remove it from engine exhausts, while CO_2 is an important greenhouse gas, which holds the potential of being utilized for the production of chemical goods. The self-assembled porous solid derived from 11 shows, however, small affinity for these compounds. For the related carbonyl sulfide (COS), the estimated affinity is very high; saturation of the pores is reached at low fugacity values. The selective recognition of carbonyl sulfide is desirable in the sweetening of natural gas.

Carbon monoxide (CO) adsorption:

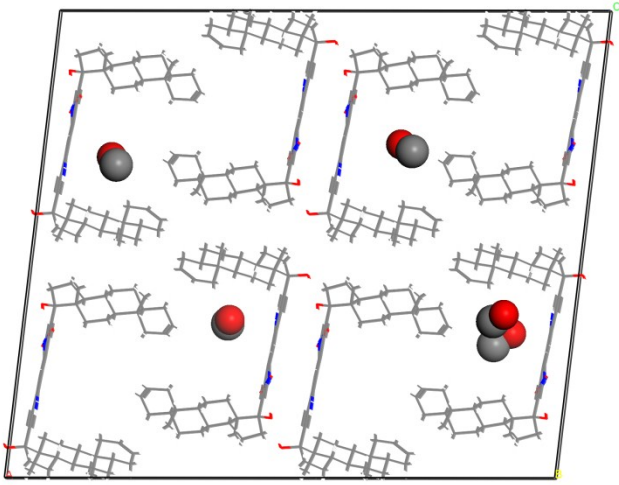

Front view of the channels present in the crystal from 11, loaded with CO

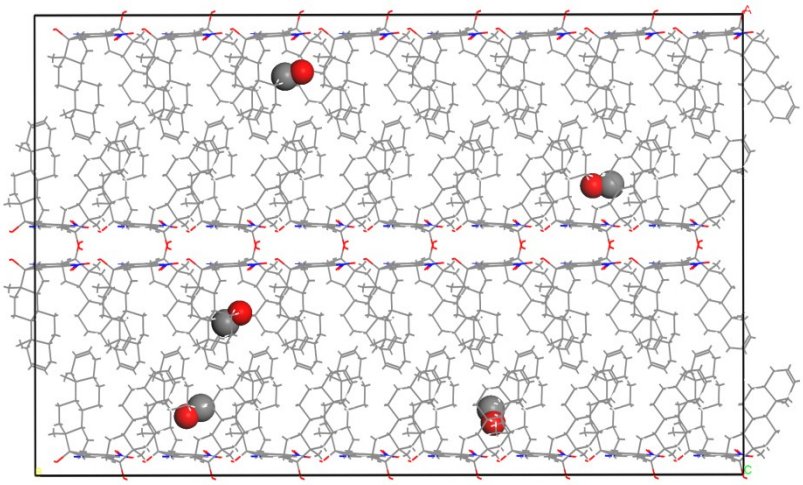

Top view of the channels present in the crystal from 11, loaded with CO

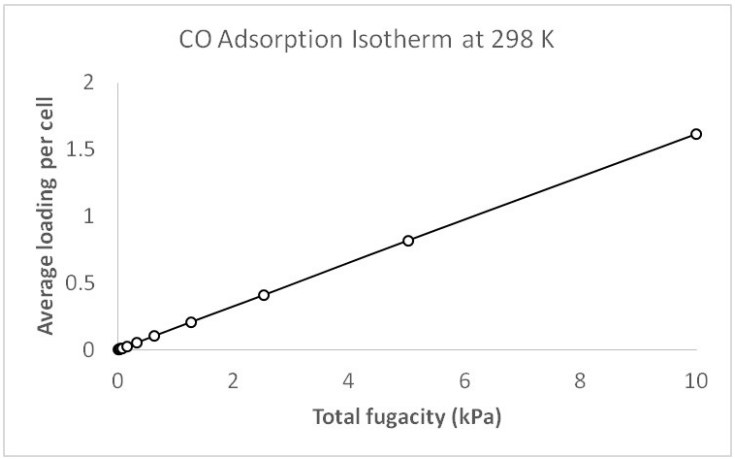

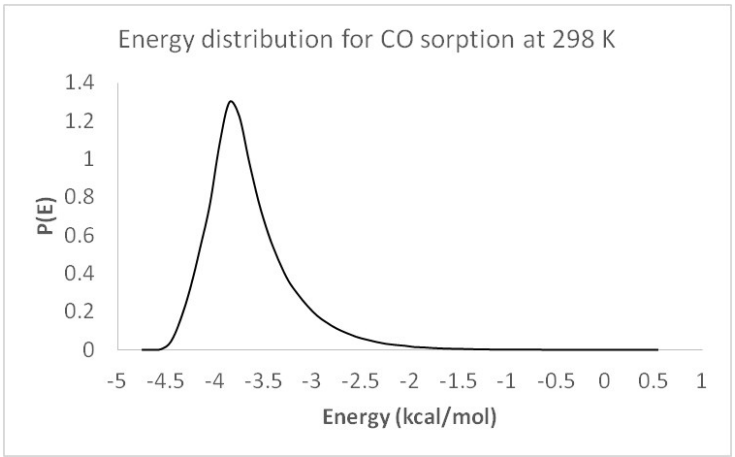

Carbon dioxide (CO_2) adsorption:

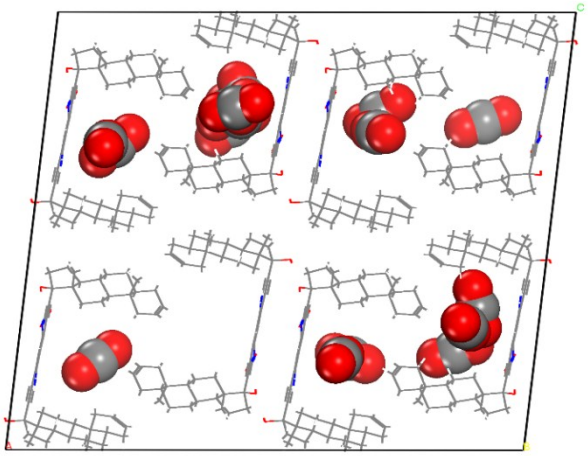

Front view of the channels present in the crystal from 11, loaded with CO_2

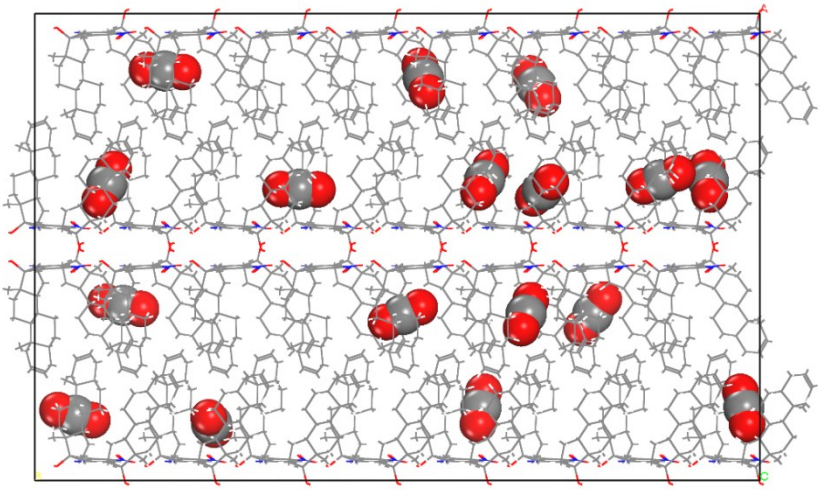

Top view of the channels present in the crystal from 11, loaded with CO_2

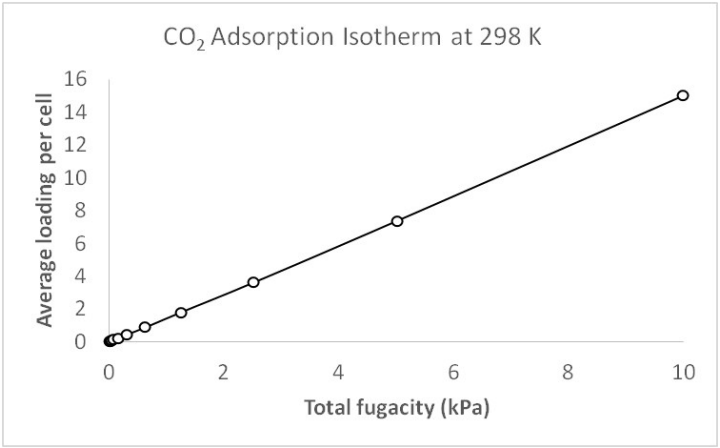

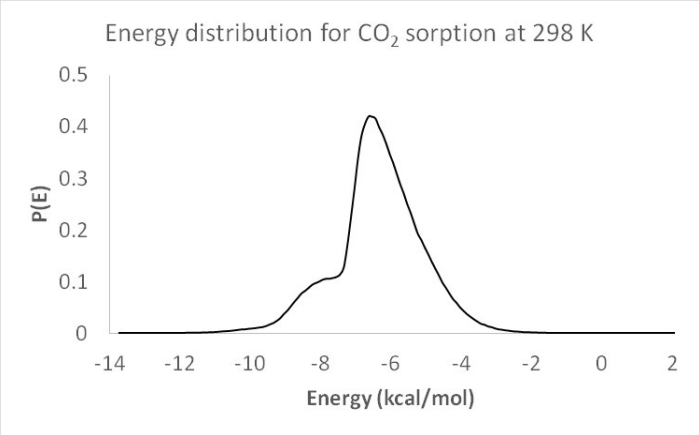

Carbonyl sulfide (COS) adsorption:

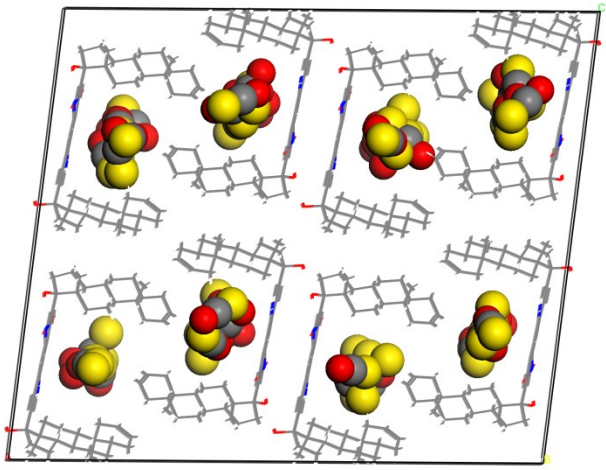

Front view of the channels present in the crystal from 11, loaded with COS

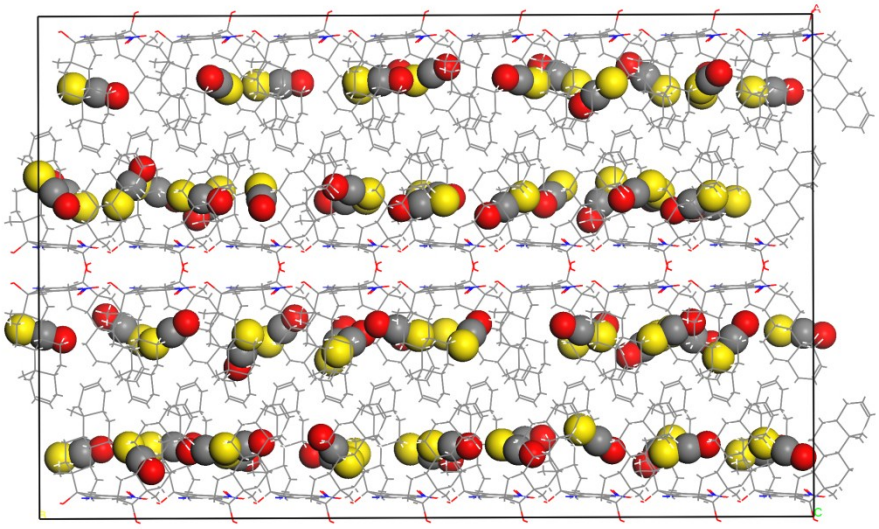

Top view of the channels present in the crystal from 11, loaded with COS